

Multimodal Assessment of Corneal Erosions Using Optical Coherence Tomography and Automated Grading of Fluorescein Staining in a Rabbit Dry Eye Model

Ifat Sher^{1,*}, Adi Tzameret^{1,2,*}, Alicja M. Szalapak³, Tomer Carmeli⁴, Estela Derazne², Noa Avni-Zauberman¹, Arie L. Marcovich^{5,6}, Guy Ben Simon^{1,2}, and Ygal Rotenstreich^{1,2}

¹ Goldschleger Eye Institute, Sheba Medical Center, Tel Hashomer, Israel

² Sackler Faculty of Medicine, Tel Aviv University, Israel

³ St John's College, University of Cambridge, Cambridge, UK

⁴ Epitech Mag LTD, 4 Hamada St, Yokneam Ilit, Israel

⁵ Department of Plant Sciences and Environmental Health, the Weizmann Institute of Science, Rehovot, Israel

⁶ Department of Ophthalmology Kaplan Medical Center, Rehovot, Israel

Correspondence: Ygal Rotenstreich, Goldschleger Eye Research Institute, Sheba Medical Center, 52621 Tel-Hashomer, Israel. e-mail: Ygal.rotenstreich@sheba.health.gov.il

Received: 11 July 2018

Accepted: 11 December 2018

Published: 28 February 2019

Keywords: SD-OCT; dry eye; corneal defects; epithelial erosions; fluorescein

Citation: Sher I, Tzameret A, Szalapak AM, Carmeli T, Derazne E, Avni-Zauberman N, Marcovich AL, Simon GB, Rotenstreich Y. Multimodal assessment of corneal erosions using optical coherence tomography and automated grading of fluorescein staining in a rabbit dry eye model. *Trans Vis Sci Tech.* 2019;8(1):27, <https://doi.org/10.1167/tvst.8.1.27> Copyright 2019 The Authors

Purpose: To evaluate the potential use of anterior segment spectral domain optical coherence tomography (AS-SD-OCT) combined with an automated grading of fluorescein staining for assessment of corneal erosions in a rabbit short-term dry eye model.

Methods: Twenty-one New Zealand white rabbits were anesthetized and eyes were kept open for 140 minutes to induce acute corneal desiccation. Rectangular scans of the cornea were performed using Spectralis AS-SD-OCT. Total corneal thickness, corneal epithelial thickness, and the percentage of epithelial erosion area (PEEA) were evaluated. Corneas were stained with fluorescein and graded automatically using EpiView and semi-automatically using ImageJ. Spearman's rank-order correlations were calculated to compare the AS-SD-OCT PEEA and the two corneal staining scores.

Results: Eye desiccation resulted in corneal epithelium erosions that covered 0.67% to 14.2% of the central cornea (mean \pm SD: 3.95% \pm 3.2%) by AS-SD-OCT. The percentage of corneal area positively stained with fluorescein ranged from 0.24% to 38.01% (mean \pm SD: 12.24% \pm 9.7%) by using ImageJ, correlating with the AS-SD-OCT PEEA (Spearman's ρ , 0.574; $P = 0.007$). The EpiView score ranged from 0.5 to 10.17 and was better correlated with the AS-SD-OCT PEEA score (Spearman's ρ , 0.795; $P = 0.000017$).

Conclusions: Our study suggests that multimodal analysis of AS-SD-OCT and grading of fluorescein staining using EpiView software may enable quantitative assessment of corneal epithelial erosions in a rabbit short-term dry eye model.

Translational Relevance: This multimodal imaging analysis may be applied for evaluation of superficial punctate keratitis associated with dry eye.

Introduction

Dry eye disease (DED) affects 5% to 6% of the world population and as high as 34% of the elderly. DED is a multifactorial disease that results in symptoms of discomfort, visual disturbance and tear film instability, tear hyperosmolarity, and chronic

damage to the corneal epithelium.¹ The severity of damage to the corneal epithelium is commonly evaluated using hydrophilic vital dyes such as sodium fluorescein.² Several grading scales have been developed. The Oxford grading scale and the National Eye Institute (NEI) grading scale are the most commonly used in clinical trials.^{3,4} The Oxford scale is based on a standard chart that defines the degree of corneal

fluorescein staining in the cornea and conjunctiva with six levels of severity.³ The NEI scale divides the cornea into five areas and the conjunctiva into six areas. Each area is given a score between 0 and 3 based on the number, size, and confluence of the punctate keratitis.⁴ Although these methods are widely used, they are subjective and highly dependent on the observer, which may lead to inter- and intraobserver variance. Several automatic algorithms have been developed for objective assessment of corneal fluorescein staining^{5–10} but to the best of our knowledge they have not been implemented in the clinic or in translational studies.

Recently, several studies reported the use of optical coherence tomography (OCT) for measurement of epithelial thickness in patients with dry eye. Using Fourier-domain OCT, Cui et al.¹¹ demonstrated that in dry eye patients the corneal epithelium was significantly thinner than normal eyes in the superior region, and that patients with severe disease presented with thinner corneal epithelium. By contrast, Francoz et al.¹² reported that no significant differences were observed in corneal epithelium thickness between dry eye patients and their age-matched controls, using spectral domain (SD)-OCT.¹²

Several animal models have been developed to study DED, mimicking different pathophysiologic mechanisms that can cause dry eye. In the short-term rabbit model developed by Fujihara et al.,¹³ lid specula are used to prevent blinking. Dry areas on the cornea are induced within a few hours that are positively stained by sodium fluorescein.¹³ This model is clinically applicable since it imitates prevalent conditions of dry eyes such as eyelid dysfunction or malposition, post ptosis repair, and blinking disorders. Recently, Wang et al.^{14,15} reported the use of SD-OCT for evaluating corneal epithelial thickness in rabbits. To the best of our knowledge, there are no reports on evaluation of epithelial thickness and assessment of the size of epithelial erosions in rabbit models of dry eye. Such assessments may be valuable as a surrogate biomarker for objective evaluation of the health of corneal epithelium in preclinical translational studies aimed at developing new treatments for DED.

In the present study we developed an automatic software for quantification of corneal fluorescein staining and evaluated the potential use of AS-SD-OCT combined with fluorescein staining for assessment of corneal erosions in a rabbit short-term dry eye model.

Materials and Methods

Animals

Twenty-one female New Zealand White (NZW) rabbits age 12 to 14 weeks were purchased from Harlan Laboratories, Israel, Rehovot, and kept until treatment at the Sheba Medical Center animal facility. All animal procedures and experiments were conducted with approval and under the supervision of the Institutional Animal Care Committee at the Sheba Medical Center, Tel-Hashomer, and conformed to recommendations of the Association for Research in Vision and Ophthalmology Statement for the Use of Animals in Ophthalmic and Vision Research.

Acute Dry Eye Model

Corneal desiccation was performed following the protocol described by Fujihara et al.¹³ with minor modifications. Briefly, rabbits were anesthetized with an intramuscular injection of ketamine (35 mg/kg) and xylazine (5 mg/kg). In each rabbit, either the right eye ($n = 13$) or the left eye ($n = 8$) was kept open using a 15-mm wire speculum for 140 minutes under controlled temperature and humidity conditions (24°C, 55% relative humidity). Then, the speculum was removed and fluorescein corneal staining was performed on the desiccated eye, immediately followed by AS-SD-OCT imaging.

Fluorescein Corneal Staining

Five microliters of 5 mg/mL sodium fluorescein (Fluoresceine; Novartis, Basel, Switzerland) were instilled on the anesthetized rabbit corneas of the desiccated eyes. The eye lids were moved gently to mimic blinking to ensure proper mixing of the fluorescein dye throughout the tear film. After 30 seconds, corneas were extensively washed with 0.9% w/v Sodium Chloride (B. Braun, Melsungen AG Germany) to prevent pooling of fluorescein. The corneas were illuminated with blue light using a fiber optic light source illuminator (Volpi AG intralux 6000, Schlieren, Switzerland) covered with a blue filter (Rosco E-COLOR+) and photographed by a digital camera (SONY digital HD video camera recorded HDR-SE12E) with the lens covered with a yellow filter (Rosco E-COLOR+). All images were taken 5 minutes after fluorescein instillation.

The extent of fluorescein corneal staining was evaluated using ImageJ (v1.48, National Institutes of Health, Bethesda, MD) and EpiView software. First

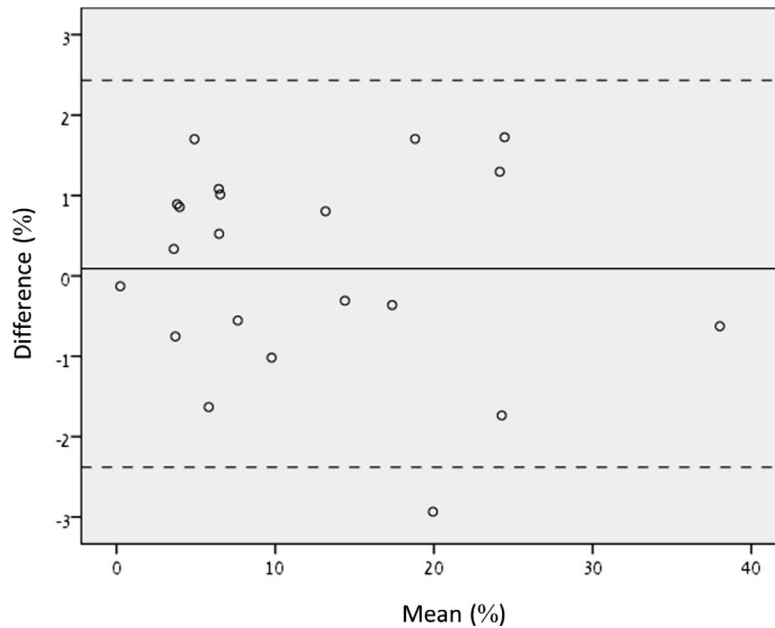


Figure 1. Bland–Altman analysis for interobserver agreement of the two readers. Bland–Altman analysis of the difference between the measurements of fluorescein positive corneal area versus the mean of the measurements taken by the two readers using ImageJ.

the area of the cornea that correlated with the AS-OCT scanned area was determined by overlaying the picture of a stained cornea with the AS-OCT image using Adobe Photoshop CC 2015 and matching the size of the eye in both images by lowering the opacity of the AS-OCT image and then aligning visible borders of the iris. The percentage of positively stained corneal area was calculated by determining the fluorescein-stained area size (in pixel) divided by the corneal area described above. The stained area was measured independently by two observers (TA, AMS). All measurements were made in a masked fashion. The agreement between the two observers was tested, following the method of Altman and Bland.¹⁶ We plotted the difference between the paired measurements against the mean value of these measurements (Fig. 1). The mean difference between the observers was $0.0893\% \pm 1.26\%$. No significant difference was found between readers ($P = 0.749$). The mean values of the measurements performed by the two observers were used for statistical analysis.

EpiView Disease State Monitoring Software

The EpiView software (Epitech Mag LTD, Israel) detects and quantifies fluorescein stained areas (“stained pixels”) within the corneal surface according to the regions defined in NEI Workshop grading system (superior, nasal, central, inferior, and temporal).⁴ For the correlation analysis, the corneal staining

score was calculated in the central cornea area, correlating with the area on which AS-SD-OCT imaging was performed (marked with a white rectangle in Fig. 1).

The analysis process consisted of the following phases:

1. Overlaying of the NEI grid over the image
2. Background subtraction, removing slow changing intensity components from the image
3. Color normalizing by multiplying the color channels by predefined factors, relative to non-stained iris color
4. Masking of pixels of concealed corneal surfaces (e.g., inner eyelid area)
5. Detection of stained pixels according to predefined range in the color space
6. Calculation of per region and total cornea Percentage of Stained Pixels [PSP] [%]
7. Calculation of per region and total cornea Mean Relative Saturation [MRS] [%]
8. The staining score calculated for this analysis was defined as total cornea $PSP \times MRS / 100$

Anterior Segment Spectral Domain Optical Coherence Tomography (AS-SD-OCT)

Spectralis Multi Color Blue Peak Spectral Domain (SD) OCT plus (Heidelberg Engineering GmbH, Heidelberg, Germany) equipped with an anterior

segment (AS) module was used to assess the anatomy of the cornea. Both eyes of all rabbits were tested at base line (prior to desiccation). The desiccated eyes were also tested immediately following fluorescein photography. Rectangular scans of the central cornea were performed with 1024 A-scans per B-scan, with a total of 21 B-scans per frame. The images were analyzed with a zoom factor of 600% to 800% provided by the SD-OCT software (Spectralis OCT; Heidelberg Engineering GmbH) with a resolution of 3.87 μm /pixel axially and 10.84 μm /pixel laterally.

Epithelial and total corneal thickness were measured using the cursors provided by the SD-OCT software. The cursors were placed perpendicular to the ocular surface epithelium from a point located just beneath the tear film (first hyperreflective layer) to the basal membrane (second hyperreflective layer). For each quadrant, three measures were obtained, and results were expressed as mean \pm SD. To evaluate percentage of epithelial erosion area (PEEA), the length of the corneal section (LCS) was measured using ImageJ software (v1.48, National Institutes of Health) and the total length of epithelial erosions (LED) in each B-scan was measured using the Spectralis OCT software (Supplementary Fig. S1). The LCS and LED from all B-scans were summed and the percentage of corneal area with epithelial erosions was calculated by the formula: AS-SD-OCT Score = Sum [LED₁₋₂₁] / Sum [LCS₁₋₂₁] \times 100. The LEDs and LCSs were measured by two observers (TA, SI). If no agreement was reached, a third observer was consulted (NAZ). All measurements were made in a masked fashion by three examiners (IS, NAZ, and AT).

Statistical Analysis

Based on preliminary data, we assumed that the mean OCT PEEA and the mean EpiView fluorescein staining score will be 3% and 3, respectively with an SD of 2.5. Assuming the data will be normally distributed, eight rabbits are required for type I error of 0.05 and type II error of 0.2. Using 21 rabbits would lead to type I error of 0.01 and type II error of 0.01. Hence, we chose a sample size of 21 rabbits. The sample size was calculated using MedCalc Version 18.10.

Kolmogorov-Smirnov and Shapiro-Wilk tests were used to determine if the data are normally distributed. Kolmogorov-Smirnov analysis demonstrated that the data of EpiView score was normally distributed but the data of OCT PEEA and ImageJ were not normally distributed. Shapiro-Wilk test demonstrated that the data of the three scores were not normally distributed. Hence, Spearman's ρ test correlation analysis was

performed to evaluate the association between the AS-SD-OCT PEEA score and corneal fluorescein staining score determined by ImageJ and EpiView.

Shapiro-Wilk test demonstrated that all data of the corneal and epithelial thickness were distributed normally, except the epithelial thickness in the left eye following desiccation. Hence, Wilcoxon rank sum test was used to assess the difference in epithelial thickness before and after desiccation in the left eye. Paired *t*-test was used to evaluate the differences in total corneal and epithelial thickness between eyes at baseline testing, total corneal thickness before and after desiccation in both eyes, and epithelial thickness before and after desiccation in the right eye. All analyses were performed using SPSS for Windows version 20.0.

Results

Detection of Epithelial Erosions Using AS-SD-OCT Imaging and Fluorescein Staining in the Rabbit Dry Eye Model

Prior to desiccation, the rabbit corneal epithelium was intact, as evident by lack of fluorescein staining (Fig. 2A). AS-SD-OCT imaging supported the lack of fluorescein staining, demonstrating no epithelial erosions in any of the tested corneas (a representative image is shown in Fig. 2B). The mean central corneal epithelium layer thickness at baseline measurement was 31.6 \pm 6 μm for OD and 30.1 \pm 4.3 μm for OS (mean \pm SD).

Following 140 minutes of desiccation, significant corneal fluorescein staining was evident, reflecting discontinuities in the tear film and damage to the corneal epithelium (Fig. 2C). Quantification of the corneal area positively stained with fluorescein ranged from 0.24% to 38.01% (mean \pm SD, 12.24% \pm 9.7%). AS-SD-OCT imaging demonstrated epithelial erosions in the areas that were positive for fluorescein staining (Fig. 2D). In these erosions, epithelium layer AS-SD-OCT thickness ranged from 26 μm to complete loss of the epithelium layer (mean \pm SD, 10.23 \pm 9.23 μm). These erosions covered 0.67% to 14.2% of the cornea (mean \pm SD, 3.95% \pm 3.2%). The PEEA as determined by AS-SD-OCT was smaller by nearly fourfolds (mean \pm SD, 3.99 \pm 2.74 folds) from the percentage of corneal area that was positive for sodium fluorescein staining as determined by ImageJ. Spearman's ρ correlation between the two scores was 0.574 (Fig. 3; $P = 0.007$). The EpiView score ranged between 0.5 and 10.17 and better correlated with the AS-SD-OCT PEEA score (Spearman's ρ , 0.795; $P = 0.000017$; Fig. 4).

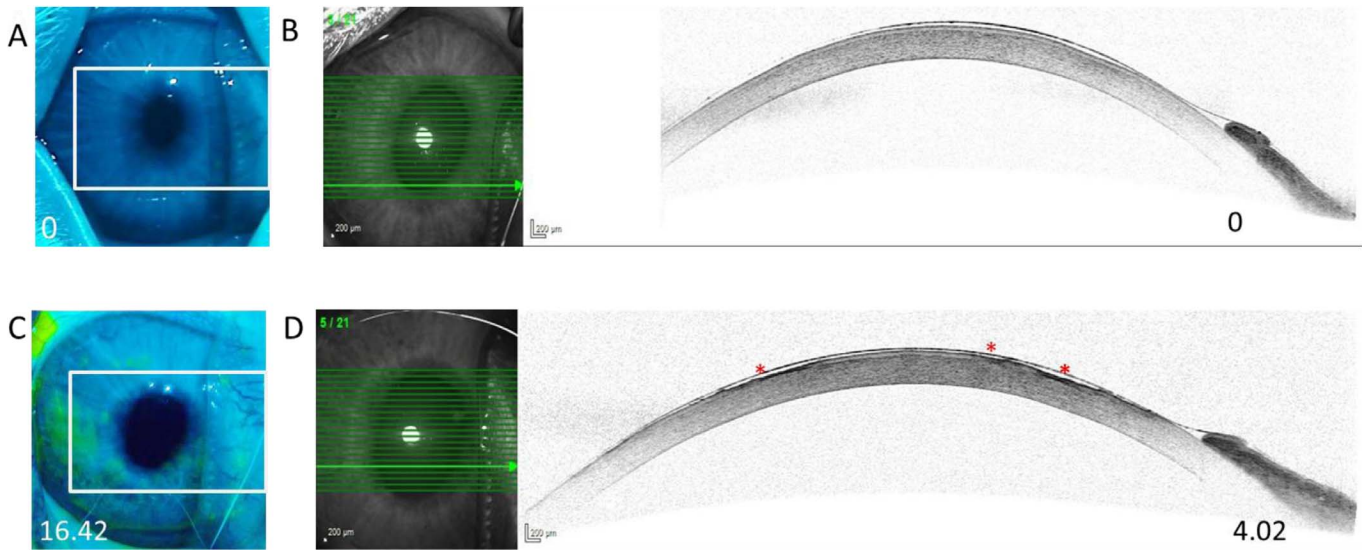


Figure 2. Corneal fluorescein staining and AS-SD-OCT imaging in a short-term dry eye rabbit model. (A), (C) Representative images of corneal fluorescein staining of rabbit corneas prior to (A) and following (C) 140 minutes desiccation. The numbers at the bottom of the pictures represent percentage of fluorescein corneal stained area as determined by ImageJ for each eye. (B), (D) AS-SD-OCT imaging of the eyes shown in panels (A), (B), respectively. The numbers at the bottom of the pictures represent the PEEA as determined by AS-SD-OCT for each eye. (D) Epithelial erosions are marked with *red asterisks*.

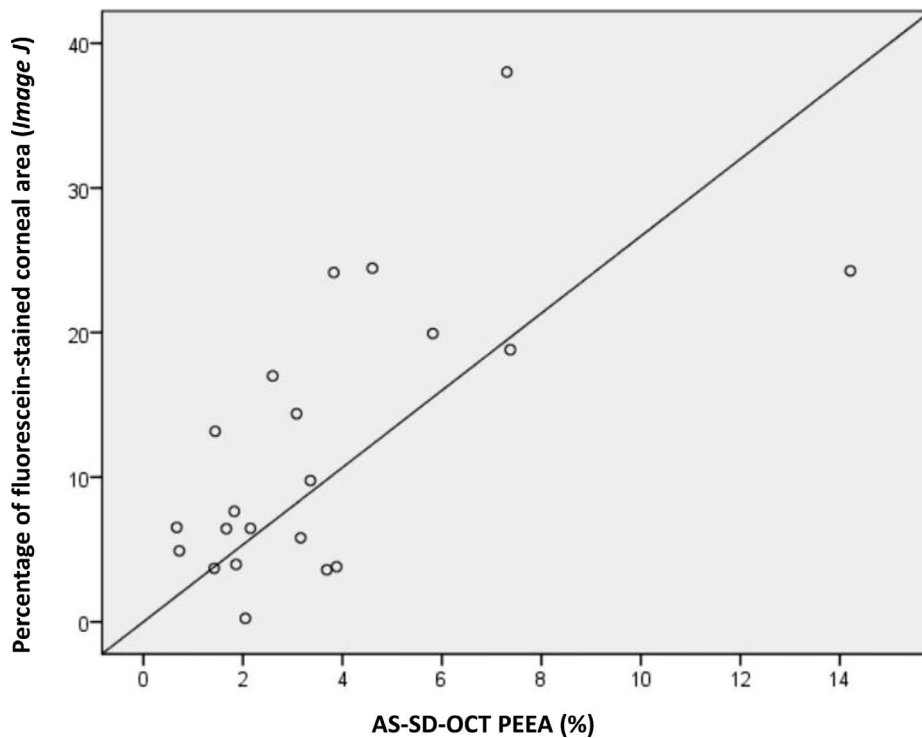


Figure 3. Correlation between the PEEA as determined by AS-SD-OCT and the percentage of corneal area positively stained with fluorescein determined by ImageJ. Positive linear correlation between the PEEA as determined by AS-SD-OCT (x-axis) and the percentage of fluorescein stained area in desiccated eyes determined by ImageJ (y-axis). *Solid line* = linear regression.

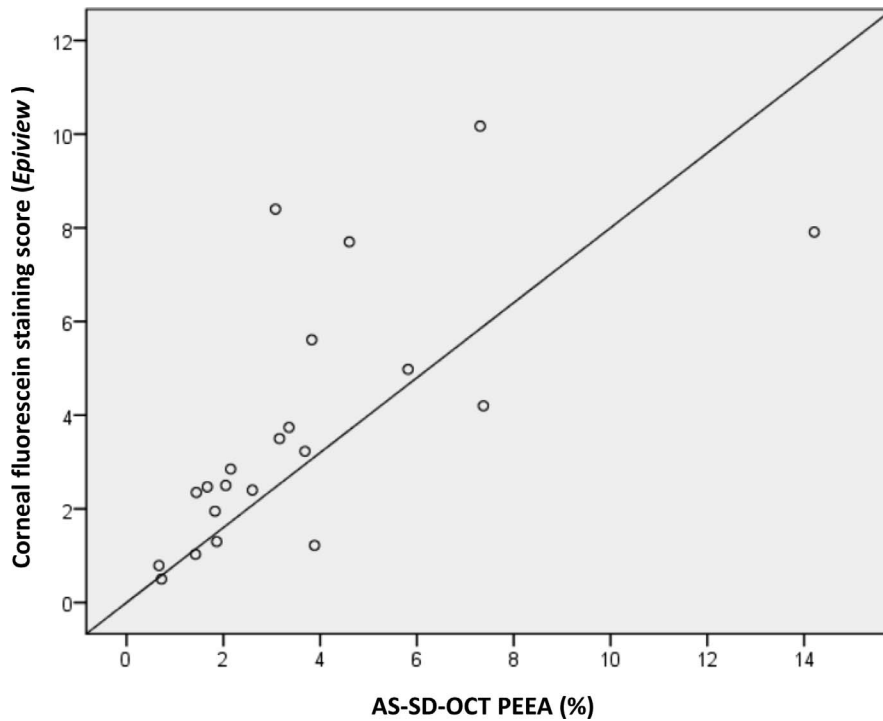


Figure 4. Correlation between the PEEA as determined by AS-SD-OCT and fluorescein staining score by EpiView software. Positive linear correlation between the PEEA as determined by AS-SD-OCT (x-axis) and the fluorescein staining score determined automatically by the EpiView software (y-axis). Solid line = linear regression.

Corneal Desiccation Has No Effect on Central Corneal AS-SD-OCT Thickness and Central Corneal Epithelial AS-SD-OCT Thickness

At baseline measurements, there were no significant differences between measurements of OD and OS for central corneal AS-SD-OCT thickness (mean \pm SD: $364 \pm 17.2 \mu\text{m}$ for OD and $370 \pm 18 \mu\text{m}$ for OS; $P = 0.321$) and central corneal epithelial AS-SD-OCT thickness ($31.6 \pm 6 \mu\text{m}$ for OD and $30.1 \pm 4.3 \mu\text{m}$ for OS; $P = 0.261$). Following desiccation, mean central corneal thickness decreased with greater variability. However, this reduction did not reach statistical significance ($349.5 \pm 27.89 \mu\text{m}$ for OD and $374 \pm 19.86 \mu\text{m}$ for OS; $P = 0.117$ and $P = 0.567$, respectively compared to baseline). Similarly, there were no significant differences in the mean SD-OCT central corneal epithelium thickness between baseline measurement and following desiccation ($29.8 \pm 4.72 \mu\text{m}$ for OD, and $29 \pm 1.07 \mu\text{m}$ for OS, P values 0.312 and 0.053, respectively).

Discussion

To the best of our knowledge, this is the first report of assessment of corneal damage in a rabbit

dry eye model using multimodal analysis of AS-SD-OCT imaging and fluorescein corneal staining. We demonstrated good correlation between corneal fluorescein staining and AS-SD-OCT epithelial erosions, specifically when the automatic scoring software EpiView was employed. Our study suggests that multimodal imaging including AS-SD-OCT and automatic quantification of corneal fluorescein may enable objective and quantitative assessment of corneal epithelial erosion size, correlating with fluorescein staining. This multimodal analysis may be applied as a surrogate marker for evaluating corneal epithelial disease, assessment of therapeutic effects and safety of new therapeutics in rabbits. In addition, this multimodal analysis may potentially be employed for evaluation of superficial punctate keratitis associated with dry eye. Clinical studies will be needed to verify the potential clinical use of this multimodal corneal imaging analysis.

The AS-SD-OCT measurements of corneal epithelium thickness presented here are supported by histology analysis demonstrating that the epithelium thickness in NZW rabbits ranges between 26.1 and 42.8 μm in 3-month-old albino rabbits.¹⁷ By contrast, Li et al.¹⁸ and Reiser et al.¹⁹ reported thicker central corneal epithelium thickness ($50.6 \pm 3.9 \mu\text{m}$

and $45.8 \pm 2.2 \mu\text{m}$, respectively) in live rabbits using confocal microscopy through-focusing methodology¹⁸ and in post mortem NZW rabbit eyes using ultrahigh resolution OCT,¹⁹ respectively. These differences may have resulted from the use of different imaging technologies and possible differences between live and post mortem sample as well as different breeds. Development of an algorithm for automatic image analysis and measurement of epithelial thickness and erosion size is predicted to improve the test accuracy.

Our measurements of baseline central corneal thickness were in agreement with those of Wang et al.¹⁵ who used Visante AS-OCT and reported a mean central corneal thickness measurement of $373 \pm 7.2 \mu\text{m}$ in NZW rabbits. After desiccation, central corneal thickness decreased with greater variability. However, this reduction did not reach statistical significance. Since corneal erosions were not necessarily in the center of the cornea, the central corneal thickness was not necessarily affected by desiccation, nor did central epithelial thickness. These findings are in agreement with the published AS-SD-OCT studies in human patients where there was no significant difference in central corneal thickness between dry eye patients and their controls.^{11,12}

In the presented study, the duration of fluorescein staining was 30 seconds followed by irrigation with BSS for at least 1 minute, which may have led to leakage under the healthy epithelium. This may explain our findings that the percentage of fluorescein stained area measured using ImageJ was larger than the area of the erosions measured by the AS-SD-OCT. Our findings are in accordance with the findings of several studies^{20–24} suggesting that epithelial cells that are programmed for shedding are stained by fluorescein.

In the presented analysis, we used ImageJ to quantify the percentage of fluorescein stained area. By contrast, the score obtained by the EpiView software integrates the area and the intensity of fluorescein staining, which led to the higher correlation observed between the EpiView score and the AS-SD-OCT PEE score.

The EpiView software presented here may facilitate objective quantification of fluorescing corneal staining in other dry eye rabbit models, and potentially in patients. In future experiments, we will examine the correlation between grading of human data by the clinicians using the NEI scoring and EpiView software, which may require the use of alternative image processing tools such as supervised machine learning classifiers (e.g., support vector machine).

Future versions of the software will cover also the conjunctiva, support alternative grading scales (e.g., the Oxford scale), staining dyes (lissamine green, rose bengal), and potentially the identification of erosions based on high definition or high dynamic range imaging.

Taken together, multimodal AS-SD-OCT and fluorescein staining analysis by the EpiView software may allow assessment of therapeutic effects of experimental interventions and better evaluation of corneal pathology in this rabbit model of acute dry eye. These objective measures minimize the subjective input from human observers, and may result in lower inter- and intragrader variability that is important in progression analysis and in translational studies aimed at evaluation of intervention safety and efficacy. As rabbits are commonly used for screening therapeutics for dry eye, this study may lead to a new surrogate outcome measures in such preclinical trials. Future studies will be aimed at assessment of the feasibility of using AS-SD-OCT and the EpiView software for monitoring corneal epithelial erosions in other dry eye animal models and punctate epithelial erosions in patients with dry eye and may serve as an objective endpoint for translational studies.

Acknowledgments

This study was supported by Epitech Mag LTD research grant (YR). Epitech Mag LTD staff participated in review of the manuscript but had no role in the design or conduct of this research.

Disclosure: **I. Sher**, Epitech Mag LTD (F), Epitech Mag Ltd 2015–2017 (E), Everads Therapy Ltd (E), EpiView software (P); **A. Tzameret**, None; **A.M. Szalapak**, None; **T. Carmeli**, Epitech Mag Ltd (E), EpiView software (P); **E. Derazne**, None; **N. Avni-Zauberman**, None; **A.L. Marcovich**, None; **G.B. Simon**, None; **Y. Rotenstreich**, Epitech Mag LTD (F), Epitech Mag Ltd 2015–2017 (E), Everads Therapy Ltd (E), EpiView software (P)

*Ifat Sher and Adi Tzameret contributed equally to this article.

References

1. The definition and classification of dry eye disease: report of the Definition and Classifica-

- tion Subcommittee of the International Dry Eye WorkShop (2007). *Ocul Surf.* 2007;5:75–92.
2. Bron AJ, Abelson MB, Ousler G, et al. Methodologies to diagnose and monitor dry eye disease. *Ocul Surf.* 2007;5:108–152.
3. Bron AJ, Evans VE, Smith JA. Grading of corneal and conjunctival staining in the context of other dry eye tests. *Cornea.* 2003;22:640–650.
4. Lemp A. Report of the National Eye Institute/ Industry Workshop on clinical trials in dry eyes. *Eye Contact Lens.* 1995;21:221–232.
5. Pritchard N, Young G, Coleman S, Hunt C. Subjective and objective measures of corneal staining related to multipurpose care systems. *Cont Lens Anterior Eye.* 2003;26:3–9.
6. Wolffsohn JS, Purslow C. Clinical monitoring of ocular physiology using digital image analysis. *Cont Lens Anterior Eye.* 2003;26:27–35.
7. Tan B, Zhou Y, Svitova T, Lin MC. Objective quantification of fluorescence intensity on the corneal surface using a modified slit-lamp technique. *Eye Contact Lens.* 2013;39:239–246.
8. Chun YS, Yoon WB, Kim KG, Park IK. Objective assessment of corneal staining using digital image analysis. *Invest Ophthalmol Vis Sci.* 2014;55:7896–7903.
9. Rodriguez JD, Lane KJ, Ousler GW, Angjeli E, Smith LM, Abelson MB. Automated grading system for evaluation of superficial punctate keratitis associated with dry eye. *Invest Ophthalmol Vis Sci.* 2015;56:2340–2347.
10. Amparo F, Wang H, Yin J, Marmalidou A, Dana R. Evaluating corneal fluorescein staining using a novel automated method. *Invest Ophthalmol Vis Sci.* 2017;58:BIO168–BIO173.
11. Cui X, Hong J, Wang F, et al. Assessment of corneal epithelial thickness in dry eye patients. *Optom Vis Sci.* 2014;91:1446–1454.
12. Francoz M, Karamoko I, Baudouin C, Labbé A. Ocular surface epithelial thickness evaluation with spectral-domain optical coherence tomography. *Invest Ophthalmol Vis Sci.* 2011;52:9116–9123.
13. Fujihara T, Nagano T, Nakamura M, Shirasawa E. Establishment of a rabbit short-term dry eye model. *J Ocul Pharmacol Ther.* 1995;11:503–508.
14. Wang X, Wu Q. Normal corneal thickness measurements in pigmented rabbits using spectral-domain anterior segment optical coherence tomography. *Vet Ophthalmol.* 2013;16:130–134.
15. Wang X, Dong J, Wu Q. Mean central corneal thickness and corneal power measurements in pigmented and white rabbits using Visante optical coherence tomography and ATLAS corneal topography. *Vet Ophthalmol.* 2014;17:87–90.
16. Altman DG, Bland JM. Measurement in medicine: the analysis of method comparison studies. *Statistician.* 1983:307–317.
17. Goes RM, Barbosa FL, Haddad A. Morphological and autoradiographic studies on the corneal and limbal epithelium of rabbits. *Anat Rec.* 2008;291:191–203.
18. Li HF, Petroll WM, Mller-Pedersen T, Maurer JK, Cavanagh HD, Jester JV. Epithelial and corneal thickness measurements by in vivo confocal microscopy through focusing (CMTF). *Curr Eye Res.* 1997;16:214–221.
19. Reiser BJ, Ignacio TS, Wang Y, et al. In vitro measurement of rabbit corneal epithelial thickness using ultrahigh resolution optical coherence tomography. *Vet Ophthalmol.* 2005;8:85–88.
20. Kikkawa Y. Normal corneal staining with fluorescein. *Exp Eye Res.* 1972;14:13–20.
21. Wilson G, Ren H, Laurent J. Corneal epithelial fluorescein staining. *J Am Optom Assoc.* 1995;66:435–441.
22. Bandamwar KL, Garrett Q, Papas EB. Mechanisms of superficial micropunctate corneal staining with sodium fluorescein: the contribution of pooling. *Cont Lens Anterior Eye.* 2012;35:81–84.
23. Bandamwar KL, Papas EB, Garrett Q. Fluorescein staining and physiological state of corneal epithelial cells. *Cont Lens Anterior Eye.* 2014;37:213–223.
24. Bron A, Argüeso P, Irkec M, Bright F. Clinical staining of the ocular surface: mechanisms and interpretations. *Prog Retin Eye Res.* 2015;44:36–61.